

---

# An Analytic Dosimetry Study for the Use of Radionuclide–Liposome Conjugates in Internal Radiotherapy

Dimitris Emfietzoglou, Kostas Kostarelos, and George Sgouros

Department of Medical Physics, University of Ioannina Medical School, Ioannina, Greece; Department of Medicine, Weill Medical College of Cornell University, New York; and Department of Medical Physics, Memorial Sloan-Kettering Cancer Center, New York, New York

---

A dosimetric analysis has been performed to evaluate the potential of liposome systems as carriers of radionuclides in internal radiotherapy. **Methods:** Pharmacokinetic data for a variety of liposome constructs (multilamellar vesicles [MLV]; small unilamellar vesicles [SUV]; and sterically stabilized liposomes, monosialoganglioside [ $G_{M1}$ ]-coated) were used to obtain tumor and normal-organ absorbed dose estimates for  $^{67}\text{Cu}$ ,  $^{188}\text{Re}$ ,  $^{90}\text{Y}$ , and  $^{131}\text{I}$ . Dosimetry was performed for two tumor models: subcutaneous Ehrlich ascites tumor, growing intramuscularly, and C26 colon carcinoma, growing intrahepatically. Dose estimates were obtained using the MIRD schema. Tumor doses were obtained assuming local deposition of electron energy; photon contributions were incorporated assuming spheric tumor geometry. With the conservative assumption that intravenously administered liposomes achieve rapid equilibration with the red marrow extracellular fluid volume, red marrow absorbed dose estimates were obtained from blood kinetics. **Results:** For intramuscular tumors, absorbed dose ratios for tumor to red marrow ranged from 0.93 ( $^{131}\text{I}$ -MLV) to 13.9 ( $^{90}\text{Y}$ -SUV). Tumor-to-liver ratios ranged from 0.08 ( $^{188}\text{Re}$ -MLV) to 0.92 ( $^{188}\text{Re}$ -SUV); corresponding values for tumor to spleen were 0.13 ( $^{90}\text{Y}$ -MLV) and 0.54 ( $^{188}\text{Re}$ - $G_{M1}$ ). The optimal combination of radionuclide and liposome system was obtained with  $^{90}\text{Y}$ -SUV. Tumor-to-liver ratios for the  $G_{M1}$ -coated construct were greatest when the tumor was intrahepatic (1.13 for  $^{90}\text{Y}$ ). For a given liposome system, absorbed dose ratios for tumor to normal tissue exhibited up to a twofold variation depending on the radionuclide selected. **Conclusion:** This study provides a dosimetric evaluation for the use of some liposome systems as carriers in targeted radionuclide therapy. Although much further work must be undertaken before any clinical application is considered, these results suggest that radionuclide targeting using liposomes is feasible and may have the advantage of reduced red marrow absorbed dose.

**Key Words:** liposomes; dosimetry; internal radiotherapy

**J Nucl Med 2001; 42:499–504**

---

**E**radication of tumors depends not solely on the cytotoxic effect of an agent but also on effective means of delivering it to the malignant site—the primary concern of targeted tumor delivery. Therapeutics can be actively targeted to particular tissues by conjugation to monoclonal antibodies, fragments of monoclonal antibodies, and other ligands with specific affinities for cellular receptors of the target tissue (e.g., folate) (1,2). Agents can be passively targeted by conjugation to colloidal particulates (e.g., for blood-pool contrast agents in nuclear medicine) (3).

Liposomes are now established delivery tools, used in many cases that require delivery of a drug, vitamin, gene, or other agent. Their unique ability to enclose and carry either hydrophilic or hydrophobic molecules in their inner aqueous phase or inside their lipid bilayer renders them useful delivery devices. Moreover, ease of manipulation of their structural and surface characteristics constitutes an extremely powerful tool of diverse physicochemical properties, which result in different pharmacokinetics. Their biocompatible, nonimmunogenic nature is considered a clinical advantage compared with other targeting and delivery modalities. Like most particulate-based pharmaceuticals, liposomes are taken up by the liver parenchymal and Kupffer's cells and drained into the spleen (4–6). Small unilamellar vesicles (SUV) (diameter < 100 nm) composed of saturated phospholipids and cholesterol are reported to have reduced uptake by the reticuloendothelial system (RES), yielding longer blood circulation half-lives compared with multilamellar vesicles (MLV) and SUV of low- or no-cholesterol molar content (7). Circulation half-lives have been further considerably improved by coating the surface of SUV with large hydrophilic groups, primarily monosialoganglioside ( $G_{M1}$ ) and polyethylene glycol (PEG) (8–10). The latter sterically stabilized liposome systems have also been reported to preferentially accumulate in solid tumors because of extravasation from the leaky endothelial barriers of tumor vasculature (11–13).

Liposomes exhibit several properties that may make liposomal delivery of radiotherapy an attractive possibility in

---

Received May 4, 2000; revision accepted Nov. 7, 2000.

For correspondence or reprints contact: George Sgouros, PhD, Department of Medical Physics, Memorial Sloan-Kettering Cancer Center, 1275 York Ave., New York, NY 10021.

specific circumstances. Unlike antibody targeting, liposomal targeting occurs at the level of the vasculature. Whereas antibodies must penetrate throughout the interstitium to reach and bind to tumor cell antigen, liposome accumulation depends primarily on enhanced vascular permeability. The widespread interstitial dissemination of radioactivity (necessary for antibody binding), followed by clearance from antigen-negative sites (necessary for antibody targeting), is not a prerequisite for liposomal targeting. Correspondingly, a resulting possible advantage is reduced residence time and, therefore, toxicity in normal organs and in particular the red marrow. Liposomal targeting is also not dependent on antigen site density and is considerably less susceptible to the impact that loading with radioactivity might have on tumor delivery. The high level of RES organ uptake seen with liposomes is perhaps the most significant known limitation of liposomal delivery systems. Preinjection strategies using liposomes that are rapidly taken up by the RES and that do not, therefore, compete with the tumor targeting systems have been used in other treatment modalities to saturate the RES and reduce liver uptake (14,15).

Conjugation of radionuclides with liposomes has been studied primarily toward development of imaging and diagnostic agents (16,17). Previous studies on the use of liposomes for delivery of radionuclides for therapy have solely focused on the chemistry of  $^{186}\text{Re}$ ,  $^{188}\text{Re}$  (18), and  $^{90}\text{Y}$  (19) conjugation to liposomes.

In this study, a dosimetric evaluation has been performed to investigate the four most widely used (experimentally and clinically) liposome types, as potential radionuclide carriers for internal radiotherapy. A first-order approximation of doses to critical tissues and model tumors was

established on the basis of animal biodistribution data of liposome systems, in combination with the emission properties of several  $\beta$ -particle emitting radionuclides:  $^{67}\text{Cu}$ ,  $^{188}\text{Re}$ ,  $^{90}\text{Y}$ , and  $^{131}\text{I}$ . Given the fundamental differences in targeting and biodistribution of liposomes relative to radioimmunoconjugates, such dosimetric analysis is an essential first step toward consideration of liposomal delivery of radionuclides to tumors.

## MATERIALS AND METHODS

### Liposomes

Experimental biodistribution data for the MLV and the SUV composed of distearoylphosphatidylcholine, cholesterol, and di-cetylphosphate (10:5:1) were extracted from Tables 1, 2, 4, and 5 and Figures 3A and B of Ogihara et al. (20). The biodistribution data for sterically stabilized liposomes prepared from distearoylphosphatidylcholine, cholesterol, and  $\text{GM}_1$  (2:1:0.2) were extracted from Figures 1A–E of Huang et al. (21). These biodistribution data are summarized in Table 1. The uncertainty of these data was generally less than 20%. All of the above described liposome systems were labeled with  $^{67}\text{Ga}$  following similar protocols, which were traced to obtain the biodistribution data. All murine xenografts were small ( $\sim 0.1$  g) at the time of intravenous administration of the liposome systems by tail vein injection; for the dosimetry calculations, tumors were scaled up using whole-body mass ratios to a size of 280 g weight and approximately 4 cm radius. Dosimetric calculations were performed for tumor, liver, spleen, kidneys, lungs, total body, and red marrow, with the latter derived from blood kinetics. The two tumor models were an Ehrlich solid tumor subcutaneously injected in the hind leg (20) and a C-26 colon carcinoma either inoculated in the left liver lobe or subcutaneously injected in the left flank (21). The types of liposomes selected represent the most widely used liposomal for-

**TABLE 1**  
Liposome Pharmacokinetics

Tissue	3 h	4 h	6 h	8 h	16 h	24 h	48 h	72 h	96 h
Tumor	1.8 (M)	8 (G)	2.0 (M)	12 (G)	18 (G)	12.6 (S)	10.6 (S)	1.2 (M)	2 (G)
	9.6 (S)	17 (G*)	14.2 (S)	24 (G*)	20 (G*)	21 (G)	8 (G)	9 (S)	4 (G*)
Liver		1.2 (G)	41.1 (M)	17 (G)	19 (G)	27.5 (M)	25.1 (M)	23.9 (M)	2 (G)
			10.2 (S)			14.9 (S)	15.5 (S)	15.1 (S)	
Spleen		21 (G)	19.6 (M)	24 (G)	27 (G)	16 (M)	10.5 (M)	10.7 (M)	8 (G)
			15.9 (S)			34.5 (S)	34.2 (S)	35.5 (S)	
Kidneys			2.2 (M)			3.74 (M)	3.1 (M)	2.9 (M)	
			4.7 (S)			5.9 (S)	4.9 (S)	5 (S)	
Lungs			1.8 (M)			2 (M)	1.4 (M)	1.5 (M)	
			4.5 (S)			2.5 (S)	1.6 (S)	1.2 (S)	
Red marrow	0.5 (M)	22.3 (G)	0.4 (M)	17.3 (G)	9.3 (G)	0.03 (M)	0.01 (M)	$9 \times 10^{-4}$ (M)	0.13 (G)
	8.2 (S)		5.1 (S)			0.6 (S)	0.04 (S)	$2 \times 10^{-3}$ (S)	
						9 (G)	1.8 (G)		

\*In liver tumor.

M = MLV; S = SUV; G =  $\text{GM}_1$ .

Data are percentage injected dose per gram of tissue.

**TABLE 2**  
Properties of Radionuclides

Radionuclide	Half-life (d)	Mean $E_{\text{particle}}$ (MeV)	Tissue $R_{\text{approx}}$ (mm)	$E_{\text{photons}}$ (MeV)
$^{131}\text{I}$	8.0	0.182 ( $\beta$ )	0.9	0.364 (81%)
$^{90}\text{Y}$	2.67	0.935 ( $\beta$ )	4.7	—
$^{67}\text{Cu}$	2.58	0.141 ( $\beta$ )	0.7	0.185 (49%)
$^{188}\text{Re}$	0.71	0.764 ( $\beta$ )	3.5	0.155 (15%)

E = energy; R = range.

mulations, which also form the basis of the three commercially available liposome formulations of anthracyclines (22).

### Radionuclides

Radionuclide selection involves the optimization of both the physical half-life and the emission properties of the radionuclide toward maximizing therapeutic effects. In this study, radionuclides with physical half-lives ranging from several hours to a few days were selected (Table 2). To investigate the optimal radionuclide–liposome combination, we studied both low- and high-energy  $\beta$ -emitters. The radionuclides,  $^{131}\text{I}$  and  $^{90}\text{Y}$ , are in widespread clinical use for radioimmunotherapy (23).  $^{67}\text{Cu}$  and  $^{188}\text{Re}$  were included because these are analogous to  $^{131}\text{I}$  and  $^{90}\text{Y}$  in their  $\beta$ -particle emission properties but have shorter half-lives.

### Dosimetry

Average tissue doses were calculated on the basis of the standard MIRD schema (24,25). The dose to the tumor from radioactivity in other organs was estimated from normal organ S-factors by setting the tumor dose equal to the dose delivered to the organ within which the tumor was contained in a standard organ geometry (e.g., liver or muscle in our model). Tumor self-dose was calculated by assuming complete absorption of electrons because the scaled-up dimensions of the tumor volume in humans (~4 cm radius) significantly exceed the range in tissue of the emitted electrons (Table 2). Edge effects may be also safely neglected for the particular tumor size and  $\beta$ -particle range (26). The contribution of photons to the tumor self-dose was estimated by tabulated absorbed fractions assuming spheric tumor geometry (27,28). Because the radioactivity from various source organs is explicitly accounted for in the formulation, and to avoid overestimation by double-counting of their dose contribution, the S-factor of the total body as a source was appropriately adjusted to represent the remaining parts of the body (29). Cumulative radioactivity values in the various organs were estimated by a piecewise numeric integration using the Mathematica software package (Wolfram Research, Inc., Champaign, IL). This method is well suited in our case, in which a limited number of data points are available, and, additionally, avoids the uncertainties of adopting a particular analytic distribution function. For extrapolating the time–activity data beyond the experimental range, we assumed that during the initial uptake phase, up to the first data point (3–4 h), accumulation was rapid (i.e., straight line fitting), whereas the clearance rate after the last data point (72–96 h) was of first-order kinetics (a single exponential was used) and was thus adjusted to smoothly join the preceding time interval. The uncertainty introduced by this extrapolation is considered to be less than the experimental errors

associated with the data. We also assumed that the tumor mass remained constant throughout the decay time and that radionuclide was not released from the radionuclide–liposome complex before radionuclide decay. Red marrow kinetics were derived from blood data using the conservative assumption that the concentration ratio between liposomes in blood and liposomes in the marrow is equal to 0.36, a value previously derived for antibodies (30). This assumption provides a worst-case assessment of red marrow absorbed dose because the size of liposomes makes them less likely to rapidly equilibrate within the marrow extracellular fluid volume. All mouse activity data were scaled up to humans by a simple relative-mass-organ correction factor; that is, the percentage injected activity at any time in a human organ was taken to be equal to the respective percentage in the animal organ multiplied by the ratio of the fraction of the total body mass of the organ in the human to the fraction in the animal (31). Inherent in this formalism is the assumption of homogeneous distribution of the radionuclide–liposome complex in the residing regions. The importance of microheterogeneity has been illustrated for other targeting agents (32). The lack of quantitative information relevant to the microdistribution of liposomes inside tumor volumes justifies, at present, the adoption of this assumption. A simple mass-ratio scaling-up from mouse to man may be inaccurate; the work is intended, however, to be an initial assessment of the potential of liposomal delivery of radionuclides for tumor targeting as well as an inter-comparison of different radionuclides and liposomal constructs. The scaling-up will minimally affect the comparison of radionuclides and liposomal constructs. Tumor and normal-organ absorbed doses derived from animal studies are likely to be different from those that would be seen in humans, however. Experience with antibodies suggests that a definitive assessment of tumor and normal-organ doses cannot be determined from animal studies and must await human studies.

### RESULTS

Figure 1 depicts tumor absorbed doses per administered activity for the four radionuclides and four liposome systems examined. Tumor absorbed dose is lowest for the MLV system regardless of radionuclide. This finding was expected because of the almost complete and rapid clearance of MLV liposomes to the liver and spleen after intravenous administration.

The importance of the emission properties of the radionuclide with respect to liposome biodistribution is clearly seen in the data of Figure 1. Even though  $^{90}\text{Y}$  and  $^{188}\text{Re}$  emit particles of similar mean energy and penetrative component (Table 2),  $^{90}\text{Y}$  delivers significantly higher doses to tumors (twofold to threefold) when conjugated to either SUV or  $G_{\text{M1}}$ . This effect is caused by their different half-lives (Table 2), indicating that the  $^{90}\text{Y}$  half-life (2.67 d) resonates better with the time frame in which liposomes reach maximum concentration within tumors (Table 1). On the other hand, for all liposome systems  $^{67}\text{Cu}$  delivers notably lower doses than  $^{90}\text{Y}$  despite their similar half-lives, because of the low  $\beta$ -energy emission of  $^{67}\text{Cu}$ . Interestingly, the biodistribution of  $G_{\text{M1}}$  liposomes results in similar tumor absorbed doses by  $^{131}\text{I}$  and  $^{188}\text{Re}$ , which have very different half-lives and emission properties. Finally, for all radionuclides,  $G_{\text{M1}}$ -

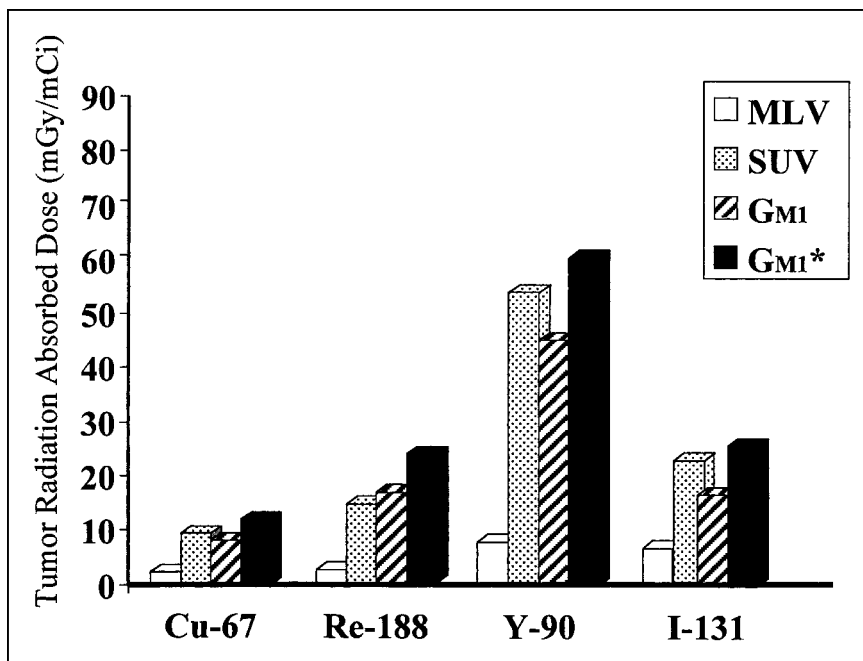


**FIGURE 1.** Tumor absorbed doses per unit administered activity for MLV, SUV, and  $G_{MI}$ -coated liposomes conjugated with (from left to right)  $^{67}Cu$ ,  $^{188}Re$ ,  $^{90}Y$ , and  $^{131}I$  (\* refers to the liver tumor model).

coated liposome delivery results in absorbed doses higher in liver tumors than in muscle tumors (black vs. gray bars in Fig. 1). These predictions are consistent with the general observation that  $G_{MI}$ -coated liposomes have been particularly effective in delivering chemotherapeutic agents to liver tumors (22). The absorbed doses per administered activity for the examined organs are presented in Table 3. The liver and spleen are the organs bearing the largest radiation burden, which is several times higher than that for the other organs.

Table 4 presents the tumor-to-normal-tissue (T/NT) absorbed dose ratios for liver, spleen, and red marrow. Except for the MLV system, the T/NT values for the kidneys and lungs were found to be much higher than 1, ranging from 2

to 7. In particular, the T/NT ratio for the total body (excluding the tumor) was between 2 and 4. Liver and spleen are common normal-organ sites of liposome localization and may, therefore, be dose limiting, whereas the red marrow is well established as the dose-limiting organ in radioimmunotherapy. Because splenectomy is not life threatening, the liver and red marrow are likely to be the dose-limiting organs. The tumor-to-red-marrow ratios (T/RM) of both  $^{90}Y$ -MLV and  $^{90}Y$ -SUV conjugates were high, but the tumor dose delivered by the MLV was too low. As seen by the tumor-to-liver ratio (T/LV), the cause was massive, rapid liver localization. In contrast, the tumor dose for  $^{90}Y$ - $G_{MI}$  is only 15% lower than that for  $^{90}Y$ -SUV, yet the T/RM ratio is much less favorable because of the prolonged

**TABLE 3**  
Tissue Radiation Absorbed Doses

Tissue	MLV				SUV				$G_{MI}$			
	$^{67}Cu$	$^{188}Re$	$^{131}I$	$^{90}Y$	$^{67}Cu$	$^{188}Re$	$^{131}I$	$^{90}Y$	$^{67}Cu$	$^{188}Re$	$^{131}I$	$^{90}Y$
Liver	0.44	0.88	0.92	2.3	0.35	0.44	0.94	1.8	0.29	0.57	0.61	1.4
Spleen	0.31	0.52	0.71	1.6	0.75	0.91	1.8	4.1	0.46	0.84	0.94	2.4
Kidneys	0.10	0.10	0.31	0.39	0.14	0.17	0.41	0.65	NA	NA	NA	NA
Lungs	0.057	0.064	0.20	0.22	0.055	0.093	0.17	0.20	NA	NA	NA	NA
Red marrow	0.051	0.058	0.20	0.017	0.068	0.12	0.21	0.11	0.16	0.35	0.34	0.51
Total body	0.11	0.15	0.32	0.53	0.11	0.15	0.30	0.50	0.11*	0.15*	0.30*	0.51*

\*Values for intrahepatic tumor.

NA = data not available.

Data are mGy/MBq.



**TABLE 4**  
Tumor-to-Normal-Tissue Radiation Absorbed Dose Ratio

Liposome system	<sup>67</sup> Cu			<sup>188</sup> Re			<sup>131</sup> I			<sup>90</sup> Y		
	T/LV	T/S	T/RM	T/LV	T/S	T/RM	T/LV	T/S	T/RM	T/LV	T/S	T/RM
MLV	0.13	0.19	1.17	0.08	0.14	1.27	0.20	0.26	0.93	0.09	0.13	12.2
SUV	0.71	0.33	3.69	0.92	0.44	3.21	0.67	0.35	2.98	0.80	0.35	13.9
G <sub>M1</sub>	0.75	0.48	1.38	0.80	0.54	1.31	0.75	0.48	1.35	0.84	0.50	2.39
G <sub>M1</sub> *	1.09	0.70	2.05	1.11	0.76	1.82	1.12	0.74	2.08	1.13	0.67	3.20

\*Intrahepatic tumor.

T/S = tumor-to-spleen ratio.

circulation half-time of G<sub>M1</sub> in blood (12.4 h compared with 5.82 h for SUV).

## DISCUSSION

Liposomes have been extensively used in tumor chemotherapy. However, their conjugation with radionuclides has been limited to applications concerning tumor detection (33,34) and, more recently, infectious site imaging (35). For such applications, their blood circulation longevity has become the single most important factor in determining their effectiveness. Thus, small and sterically stabilized liposomes (e.g., G<sub>M1</sub>- and PEG-coated), exhibiting the longest circulation residence times so far, have been the liposome systems most commonly used clinically.

This study offers an analytic dosimetry evaluation of various liposome-radionuclide complexes. Consistent with the previously noted importance of liposome size (5,10), estimated tumor absorbed doses improved with decreasing mean liposome diameter. The shift from MLV (>1 μm mean diameter) to SUV (<100 nm mean diameter) structures significantly improved both tumor doses and T/NT values. Contrary to chemotherapeutic and imaging applications, though, the dosimetry analysis showed that SUV may well exhibit more favorable kinetics than do G<sub>M1</sub>-coated liposomes for radionuclide therapy. Red marrow toxicity is not as critical a factor in chemotherapy because it may be modulated to a greater extent than radiotherapy through the prolonged therapeutic schedules and the opportunity to adjust dose during treatment. Also, in contrast to chemotherapy, delivery of radiation absorbed dose does not require release of the drug from the liposome but, rather, can occur if the liposome-encapsulated radionuclide is in the vicinity of red marrow, as defined by the range of the radionuclide emissions. Therefore, aside from liver and RES localization, red marrow toxicity will critically determine feasibility. As this study illustrates, the long-circulating liposomes (G<sub>M1</sub>- or PEG-coated), while enhancing tumor localization, also deposit a significantly higher dose to the red marrow, thus rendering this liposome system less optimal for radiotherapy than the more quickly deposited SUV.

<sup>90</sup>Y-SUV yielded the optimal predicted radionuclide-liposome combination. <sup>90</sup>Y-SUV liposomes have already

been constructed (19). Using this combination, a liver tolerance dose of 25 Gy (5% complication in 5 y (36)) would require an administered activity of 13.4 GBq (363 mCi) and would yield a mean tumor absorbed dose of 20 Gy and 1.4 Gy to the red marrow. The red marrow absorbed dose delivered from such an administration is below the levels generally associated with dose-limiting toxicity (37). T/LV ratios may be considerably improved by preadministration of liposomes that will rapidly saturate the RES and will not compete for tumor localization with targeted liposomes (35). Moreover, tumor retention may be enhanced by the incorporation of tumor-targeting moieties on the surface of the liposome constructs (38).

## CONCLUSION

A first-order dosimetric assessment of tumor therapy using radiolabeled liposomes suggests that adequate tumor targeting and dose delivered to tumors may be achieved before normal tissue toxicity. Unlike the case with radioimmunotherapy, the dose-limiting organ is likely to be the liver, and strategies intended to reduce RES accumulation are needed to further improve such a tumor-targeting approach. The current analysis suggests that the optimal liposomal system for radiotherapy differs from that considered optimal for chemotherapeutic delivery.

## ACKNOWLEDGMENTS

This study was supported, in part, by R01CA62444 and R01CA72683 from the National Institutes of Health and BC996563 from the Army Breast Cancer Research Program.

## REFERENCES

- Buchsbaum DJ. Experimental approaches to increase radiolabeled antibody localization in tumors. *Cancer Res.* 1995;55(suppl):5729s-5732s.
- Mathias CJ, Wang S, Waters DJ, Turek JJ, Low PS, Green MA. Evaluation of <sup>111</sup>In-DTPA-folate as a potential folate-receptor-targeted radiopharmaceutical. *J Nucl Med.* 1998;39:1579-1585.
- Goins B, Phillips WT, Klipper R. Blood-pool imaging using technetium-99m labeled liposomes. *J Nucl Med.* 1996;37:1374-1379.
- Senior JH. Fate and behavior of liposomes in vivo: a review of controlling factors. *Crit Rev Ther Drug Carrier Syst.* 1987;3:123-193.
- Schwendener RD, Lagocki PA, Rahman YE. The effects of charge and size on the

- interaction of unilamellar liposomes with macrophages. *Biochim Biophys Acta*. 1984;772:93–101.
6. Moghimi SM, Porter CJH, Illum L, Davis SS. The effect of poloxamer-407 on liposome stability and targeting to bone marrow: comparison with polystyrene microspheres. *Int J Pharm*. 1991;68:121–126.
  7. Semple SC, Chonn A, Cullis PR. Influence of cholesterol on the association of plasma proteins with liposomes. *Biochemistry*. 1996;35:2521–2525.
  8. Allen TM, Chonn A. Large unilamellar liposomes with low uptake into the reticuloendothelial system. *FEBS Lett*. 1987;223:42–46.
  9. Gabizon A, Papahadjopoulos D. Liposome formulations with prolonged circulation time in blood and enhanced uptake by tumors. *Proc Natl Acad Sci USA*. 1988;85:6949–6953.
  10. Mori LD, Huang L. Role of liposome size and RES blockade in controlling biodistribution and tumor uptake of GM1-containing liposomes. *Biochim Biophys Acta*. 1992;1104:95–101.
  11. Huang SK, Martin FJ, Jay G, Vogel J, Papahadjopoulos D, Friend DS. Extravasation and transcytosis of liposomes in Kaposi's sarcoma-like dermal lesions of transgenic mice bearing the HIV tat gene. *Am J Pathol*. 1993;143:10–14.
  12. Wu NZ, Da D, Rudoll TL, Needham D, Whorton AR, Dewhirst MW. Increased microvascular permeability contributes to preferential accumulation of stealth liposomes in tumor tissue. *Cancer Res*. 1993;53:3765–3770.
  13. Yuan F, Leunig M, Huang SK, Berk DA, Papahadjopoulos D, Jain RK. Microvascular permeability and interstitial penetration of sterically stabilized (stealth) liposomes in a human tumor xenograft. *Cancer Res*. 1994;54:3352–3356.
  14. Harashima H, Sakata K, Kiwada H. Distinction between the depletion of opsonins and the saturation of uptake in the dose-dependent hepatic uptake of liposomes. *Pharm Res*. 1993;10:606–610.
  15. Wolff G, Worgall S, van Rooijen N, Song WR, Harvey BG, Crystal RG. Enhancement of in vivo adenovirus-mediated gene transfer and expression by prior depletion of tissue macrophages in the target organ. *J Virol*. 1997;71:624–629.
  16. Turner AF, Presant CA, Proffitt RT, Williams LE, Winson DW, Werner JL. In-111-labeled liposomes: dosimetry and tumor depiction. *Radiology*. 1988;166:761–765.
  17. Woodle MC. <sup>67</sup>Gallium-labeled liposomes with prolonged circulation: preparation and potential as nuclear imaging agents. *Nucl Med Biol*. 1993;20:149–155.
  18. Hafeli U, Tiefenauer LX, Schubiger PA, Weder HG. A lipophilic complex with <sup>186</sup>Re/<sup>188</sup>Re incorporated in liposomes suitable for radiotherapy. *Nucl Med Biol*. 1991;18:449–454.
  19. Utkhede D, Yeh V, Szucs M, Tilcock C. Uptake of yttrium-90 into lipid vesicles. *J Liposome Res*. 1994;4:1049–1061.
  20. Ogihara I, Kojima S, Jay M. Tumor uptake of <sup>67</sup>Ga-carrying liposomes. *Eur J Nucl Med*. 1986;11:405–411.
  21. Huang SK, Mayhew E, Gilani S, Lasic DD, Martin FJ, Papahadjopoulos D. Pharmacokinetics and therapeutics of sterically stabilized liposomes in mice bearing C-26 colon carcinoma. *Cancer Res*. 1992;52:6774–6781.
  22. Drummond DC, Meyer O, Hong K, Kirpotin DB, Papahadjopoulos D. Optimizing liposomes for delivery of chemotherapeutic agents to solid tumors. *Pharmacol Rev*. 1999;51:691–743.
  23. Larson SM, Macapinlac HA, Scott AM, Divgi CR. Recent achievements in the development of radiolabeled monoclonal antibodies for diagnosis, therapy and biologic characterization of human tumors. *Acta Oncol*. 1993;32:709–715.
  24. Snyder WS, Ford MR, Warner GG, Watson SB. "S" Absorbed Dose per Unit Cumulated Activity for Selected Radionuclides and Organs. *MIRD Pamphlet No. 11*. New York, NY: Society of Nuclear Medicine; 1975.
  25. Stabin MG. MIRDose: personal computer software for internal dose assessment in nuclear medicine. *J Nucl Med*. 1996;37:538–546.
  26. Meredith RF, Johnson TK, Plott G, et al. Dosimetry of solid tumors. *Med Phys*. 1993;20:583–592.
  27. Brownell G, Ellett W, Reddy R. MIRD pamphlet no. 3: absorbed fractions for photon dosimetry. *J Nucl Med*. 1968;27(suppl):28–39.
  28. Ellett W, Humes R. MIRD pamphlet no. 8: absorbed fractions for small volumes containing photon-emitting radioactivity. *J Nucl Med*. 1972;13(suppl):26–32.
  29. Coffey JL, Watson EE. Calculating dose from remaining body activity: a comparison of two methods. *Med Phys*. 1979;6:307–308.
  30. Sgouros G. Bone marrow dosimetry for radioimmunotherapy: theoretical considerations. *J Nucl Med*. 1993;34:689–694.
  31. Sparks RB, Aydogan B. Comparison of the effectiveness of some common animal data scaling techniques in estimating human radiation dose. In: S.-Stelson AT, Stabin MG, Sparks RB, eds. *Sixth International Radiopharmaceutical Dosimetry Symposium*. Oak Ridge, TN: Oak Ridge Associated Universities; 1996:705–716.
  32. Makrigiorgos GM, Ito S, Baranowska-Kortylewicz J, et al. Inhomogeneous deposition of radiopharmaceuticals at the cellular level: experimental evidence and dosimetric implications. *J Nucl Med*. 1990;31:1358–1363.
  33. Presant CA, Proffitt RT, Turner AF, et al. Successful imaging of human cancer with radiolabeled phospholipid vesicles (liposomes). *Cancer*. 1988;62:905–911.
  34. Stewart JS, Harrington KJ. Biodistribution and pharmacokinetics of stealth liposomes in patients with solid tumors. *Oncology*. 1997;11(suppl):33–37.
  35. Boerman OC, Storm G, van Oyen W, et al. Sterically stabilized liposomes labeled with <sup>111</sup>In to image focal infection in rats. *J Nucl Med*. 1995;36:1639–1644.
  36. Bentel GC, Nelson CE, Noell KT. *Treatment Planning and Dose Calculation in Radiation Oncology*. 4th ed. Elmsford, NY: Pergamon Press; 1989:4.
  37. Sgouros G, Divgi CR, Scott AM, Williams J, Larson SM. Hematologic toxicity in radioimmunotherapy: an evaluation of different predictive measures [abstract]. *J Nucl Med*. 1996;37(suppl):43P–44P.
  38. Mathias CJ, Hubers D, Low PS, Green MA. Synthesis of [<sup>99m</sup>Tc]DTPA-folate and its evaluation as a folate-receptor-targeted radiopharmaceutical. *Bioconjug Chem*. 2000;11:253–257.